PERGAMON

International Journal of Heat and Mass Transfer 43 (2000) 1391–1398

International Journal of HEAT and MASS TRANSFER

www.elsevier.com/locate/ijhmt

Condensation on the outside surface of a small/mini diameter tube for vapor flowing through a horizontal annulus surround by an adiabatic concentric tube

Bu-Xuan Wang*, Xiao-Ze Du

Thermal Engineering Department, Tsinghua University, Beijing 100084, People's Republic of China

Received 23 April 1999; received in revised form 25 June 1999

Abstract

An analytical model, simultaneously accounting for gravity, vapor shear along axial direction and surface tension effects on the condensate film layer, is proposed for flow condensation process in horizontal annulus with small/mini diameter inner tube and traditional industrial-used outer adiabatic tube. The analysis shows that, the effect of surface tension can not be neglected for small/mini tube of diameter less than 3 mm o.d., especially in low vapor quality zone. The shear stress and surface tension influence the flow condensation mainly by means of distributing condensate film uniformly along tube circumference in horizontal annulus. Experiments were conducted to examine the analysis.

Keywords: Flow condensation; Outside of small/mini tube; Theoretical analysis; Experimental examination

1. Introduction

Flow condensation is widely adopted in process industries, refrigeration equipment, and power system. As a result of technological progress, it is essential to have compact and efficient condensers in many applications, such as automotive air conditioners or life-support systems in space, and also the recent advances for micro mechanical system (MMS). It is therefore logical to use small or mini-diameter tubes. We can deduce that more efficient condensation will take place inside or outside a pipe of small/mini diameter owing to larger specific surface area for heat transfer. In the present study, an assessing of the potential of such a horizontal annulus as condenser with inner small/mini diameter tube is taken.

Up to now, the Nusselt analysis [1] for laminar film condensation is still used as the fundamental basis for solving problems connected with condensation. However, there are many circumstances where Nusselt theory underpredicts the heat transfer rate. This results from the basic assumptions Nusselt obtained his solution on plain surfaces for the case of non-moving vapor and neglecting the shear stress on vapor–liquid interface. Many attempts [2–4] have been done to improve Nusselt's analysis by taking into account the effect of shear stress. However, few have taken into consideration the surface tension effects on the condensate film in their analysis. Rohsenow [5] put forward that for tubes of diameter larger than 3 mm, the con-

* Corresponding author. Tel.: +86-10-6278-4530; fax: +86-10-6277-0209.

E-mail address: bxwang@mail.tsinghua.edu.cn (B.-X. Wang).

0017-9310/00/$ - see front matter
PII: S0017-9310(99)00228-8

Nomenclature

c_f	friction coefficient
D	inside diameter of outer tube
d	outside diameter of inner tube
g	gravitational acceleration
h_{lv}	latent heat of condensation
$\dot{m}$	mass flow rate
Nu	Nusselt number
p	pressure
q	heat flux
R	outside radius of inner tube
Re	Reynolds number
r	radial coordinate
T	temperature
u	velocity in axial direction
v	velocity along circumference
x	vapor quality
z	axial coordinate

Greek symbols

α	heat transfer coefficient
δ	thickness of condensate film
λ	thermal conductivity
μ	dynamic viscosity
θ	polar angle
ρ	density
σ	surface tension
τ	shear stress

Subscripts

0	inlet
cool	cooling water
exp	experimental
i	inner tube
l	liquid
o	outer tube
R	ratio of liquid and vapor properties
s	saturation state
v	vapor
w	tube wall
δ	vapor–liquid interface

Superscript

-	average or mean value

densate film can be treated as on a plain surface, otherwise, the bending effect of condensate film can not be neglected. Some researchers have reported the impact of surface tension on the curved condensate surface, primarily with respect to leading edge effects [6–8]. Krupiczka [9] and Buznik et al. [10] considered the variation in curvature of condensate film, accounted for a pressure gradient term due to surface tension. Jacobi and Goldschmidt [11] extended Nusselt's analysis to discuss the Marangoni effect on film-wise condensation heat transfer around a cylinder in cross flow. Most of these studies quoted [6–11] focused on the condensation for vapor cross flow on a cylinder and didn't attempt to account for the coupling effects of shear stress in tube axial direction.

The purpose of present study is to simultaneously account for gravity, vapor shear along axial direction and surface tension effects on the condensate layer in horizontal concentric annulus with cold small/mini-diameter inner tube and an adiabatic outer wall. Flow condensation outside along a traditional inner tube of larger diameter is also reckoned as for comparison.

2. Theoretical analysis

Taking the cylindrical co-ordinate system shown in Fig. 1, a horizontal annulus with uniform temperature T_w of inner wall surface and adiabatic outer wall is considered. The saturated vapor at temperature T_s, which is greater than T_w, flows in the annulus with inlet Reynolds number Re_{v0} and is condensed on the inner tube wall surface. The condensate film is simultaneously drained by shear stress due to the vapor flow in axial direction, dz, and by either gravity or surface tension in circumference direction, $r \cdot d\theta$, respectively.

The simplifying assumptions are made as: (1) there are no interfacial waves between the condensate and vapor; (2) there is no presence of non-condensable gas; (3) neglect the convective terms in energy equation and the inertia terms of momentum equation; (4) the temperature of the outer surface of the film was the same

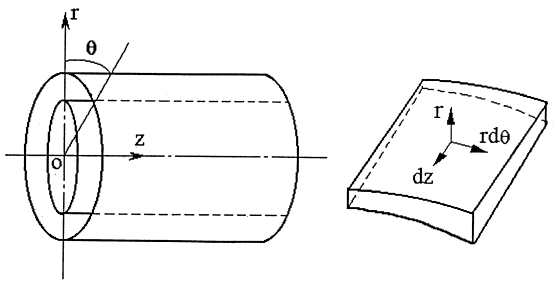

Fig. 1. Coordinating system and elementary condensate film volume for analysis.

as the saturated vapor temperature; (5) the density, ρ_l, thermal conductivity, λ_l, and viscosity, μ_l, of the condensate are taken as constants, being independent of temperature.

Then, the governing equations for conservation of mass flow and momentum transfer across the condensate film will be:

$$\frac{1}{r}\frac{\partial v}{\partial \theta}+\frac{\partial u}{\partial z}=0 \tag{1}$$

where v is the condensate film velocity along circumference, u is the velocity along axial direction, and

$$\mu_l\frac{\partial^2 v}{\partial r^2}+\rho_l g\ \sin\ \theta-\frac{1}{r}\frac{\partial p_l}{\partial \theta}=0 \tag{2}$$

with the corresponding boundary conditions:

$$v=0,\quad \text{for}\quad r=R; \tag{3a}$$

$$\frac{\partial v}{\partial r}=0,\quad \text{for}\quad r=R+\delta_l \tag{3b}$$

where R is the outside radius of the inner tube, δ_l is the condensate film thickness, or $\delta_l=f(r,\ \theta)$. In axial direction, we have

$$\frac{1}{r}\frac{\partial}{\partial r}\left(r\mu_l\frac{\partial u}{\partial r}\right)+\rho_l g-\frac{\partial p_l}{\partial z}=0 \tag{4}$$

with boundary conditions as:

$$u=0,\quad \text{for}\quad r=R \tag{5a}$$

$$\mu_l\frac{\partial u}{\partial r}=\tau_\delta,\quad \text{for}\quad r=R+\delta_l \tag{5b}$$

τ_δ is the shear stress on the vapor–liquid interface due to vapor flow.

The liquid film thickness will vary along the axial and circumference direction. An additional pressure gradient can be produced by surface tension due to the variation of condensate film curvature. That is,

$$p_l=p_v+\frac{\sigma}{R+\delta_l}$$

or

$$\frac{\partial p_l}{r\partial \theta}=\frac{\partial p_v}{r\partial \theta}-\frac{\sigma}{(R+\delta_l)^2}\frac{\partial (R+\delta_l)}{r\partial \theta} \tag{6}$$

we have

$$\frac{\partial p_l}{r\partial \theta}=\rho_v g\ \sin\ \theta-\frac{\sigma}{(R+\delta_l)^2}\frac{\partial (R+\delta_l)}{r\partial \theta} \tag{7}$$

if neglecting the frictional pressure drop and inertia pressure drop along the periphery.

Combined with the boundary conditions, integrating Eq. (2), we obtain the velocity profile along circumference as

$$\begin{aligned} v=&\frac{A}{\mu_l}\left[\frac{R^2-r^2}{2}+(R+\delta_l)(r-R)\right]\\ &+\frac{B}{\mu_l}\left(R\ \ln\frac{R}{R+\delta_l}-r\ \ln\frac{r}{R+\delta_l}-R+r\right)\end{aligned} \tag{8}$$

where

$$A=(\rho_l-\rho_v)g\sin\theta\quad\text{and}$$

$$B=\frac{\sigma}{(R+\delta_l)^2}\frac{\partial (R+\delta_l)}{\partial \theta} \tag{9}$$

The first term of the right-hand side of Eq. (8) results from the gravity, whereas the second term involving B reflects the effect of surface tension on vapor–liquid interface.

The film thickness in axial direction is fairly uniform as compared with the variation along circumference, and therefore, the capillary pressure drop along axial direction can be neglected. Hence, the pressure gradient of condensate film respected to z comes mainly from frictional pressure drop due to the vapor flow. A momentum balance for the vapor region yields

$$\frac{\partial p_v}{\partial z}=-\frac{2\int_0^{2\pi}\tau_\delta(R+\delta_l)\mathrm{d}\theta+\pi D_i\tau_w}{\int_0^{2\pi}[D_i/2-(R+\delta_l)]\mathrm{d}\theta}. \tag{10}$$

The condensate film thickness is comparatively so small, with respect to the hydraulic diameter of the annulus, (D_i-d_o), that, the pressure drop of liquid along axis can be obtained as

$$\frac{\partial p_l}{\partial z}=-\frac{4(\tau_\delta d_o+\tau_w D_i)}{D_i^2-d_o^2}. \tag{11}$$

No mass transfer exists on the adiabatic outer wall of the annulus, the shear stress would be resulted from the flow friction, i.e.

$$\tau_w=\frac{c_f}{2}\rho_v u_v^2. \tag{12}$$

But also, the interfacial shear stress, τ_δ, due to the vapor condensed onto liquid surface should be included on the inner wall as

$$\tau_\delta=\frac{c_f}{2}\rho_v(u_v-u\,|_{r=R+\delta_i})^2+\frac{\partial^2 m_l}{r\partial\theta\partial z}(u_v-u\,|_{r=R+\delta_l}) \tag{13}$$

among which, the two-phase flow friction coefficient,

c_f, was given by Henstock and Hamratty [12] for circular pipe flow with $Re_{v0} \geq 2000$, and was later adopted by Faghri and Chow [13] to annular flow as

$$c_f/2 = (c_f/2)^*(1 + 850F) \tag{14}$$

where

$$(c_f/2)^* = 0.085/Re_v^{0.25} \tag{15a}$$

$$F = \gamma\mu_R/(\rho_R^{0.5} Re_v^{0.9}) \tag{15b}$$

$$\gamma = [(1.414Re_l^{0.5})^{2.5} + (0.132Re_l^{0.9})^{2.5}]^{0.4}. \tag{15c}$$

Consequently, the velocity profile in axial direction can be deduced from integrating Eq. (4) along with the boundary conditions, Eq. (5), and applying Eq. (11)–(13) as

$$u = \frac{A}{2\mu_l} r^2 + \frac{C_1}{\mu_l} \ln r + C_2 \tag{16}$$

where

$$A = \frac{1}{2}\frac{dp_l}{dz} \tag{17a}$$

$$C_1 = (R + \delta_l)[\tau_\delta - A(R + \delta_l)] \tag{17b}$$

$$C_2 = -\frac{A}{2\mu_l} R^2 - \frac{C_1}{\mu_l} \ln R \tag{17c}$$

The heat conducted, through the film to the incremental element $dz \cdot r\, d\theta$ in Fig. 1, causes a change of condensate flow as

$$\lambda_l \frac{T_s - T_w}{\ln\dfrac{R+\delta_l}{R}} \frac{dz \cdot r\, d\theta}{R+\delta_l} = \rho_l h_{lv}\left[\frac{\partial}{\partial z}\left(\int_R^{R+\delta_l} u\, dr \cdot r\, d\theta\right)dz + \frac{\partial}{r\partial\theta}\left(\int_R^{R+\delta_l} v\, dr \cdot dz\right) r\, d\theta\right] \tag{18}$$

where λ_l is the conductivity of condensate film, h_{lv} is the latent heat of condensation. Then, the mass flow rate of condensate, $\dot{m}_l$, at axial position z can be acquired by

$$\dot{m}_l = \frac{\lambda_l(T_s - T_w)}{h_{lv}} \int_0^z dz \int_0^{2\pi} \ln\frac{R}{R+\delta_l} \frac{1}{R+\delta_l} r\, d\theta. \tag{19}$$

For the known inlet vapor mass flow rate, $\dot{m}_{v0}$, by the prescribed inlet vapor Reynolds number, Re_{v0}, and the hydraulic diameter of the annulus, we can determine the average vapor velocity, u_v, and vapor quality, x, at different axial position, z, from the mass balance for vapor–liquid system, i.e.

$$u_v = \frac{\dot{m}_{v0} - \dot{m}_l}{\rho_l \int_0^{2\pi} (R + \delta_l)\, d\theta} \tag{20}$$

and

$$x = \frac{\dot{m}_{v0} - \dot{m}_l}{\dot{m}_{v0}}. \tag{21}$$

Assuming a linear temperature profile in the thin condensate film, we have the local film thickness, δ_l, as

$$\alpha(z, \theta) = \frac{\lambda_l}{R \ln\dfrac{R+\delta_l}{R}}. \tag{22}$$

The average heat transfer coefficient along the periphery can be thereby predicted as

$$\bar{\alpha}(z) = \frac{1}{\pi}\int_0^\pi \alpha(z, \theta)\, d\theta \tag{23}$$

with mean Nusselt number, Nu, as

$$Nu = \frac{\bar{\alpha}(z) \cdot d_o}{\lambda_l}. \tag{24}$$

This proposed analytical model can be solved numerically. The discretizations of governing equations were taken along axis and periphery, respectively. The step size in z direction was $\Delta z = 0.1R$, while the step size taken in circumference direction was $\Delta\theta = 1°$. Using the last calculated vapor velocity u_v, shear stress τ_δ, τ_w, and prescribed condensate film thickness, which is assumed uniform in every grid, the momentum conser-

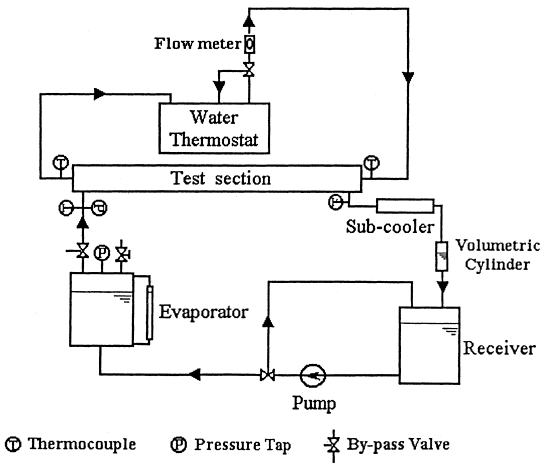

Fig. 2. Schematic diagram of the test apparatus.

vation equation was solved to determine the value of liquid mass flux. If it is not satisfied with the mass flow rate calculated from the energy conservation Eq. (19), the value of film thickness is changed slightly and the same iterative process is repeated until the relative discrepancy is less than 0.1%. After all the values of δ_l, m_l, x, u_v, τ_δ, τ_w and α are thus calculated at a cross section, the iteration is started at the next axial location.

3. Experimental examination

Experiments were conducted to examine the predicted results. The experimental apparatus is shown in Fig. 2. Water steam was used for test fluid.

The test setup consists of two main loops, namely, the vapor–condensate and cooling water loops. The cleaned water stored in the receiver is pumped into the evaporator. The by-pass line at the discharge side of the pump enables to regulate the liquid volume in the evaporator. The evaporator is an electric boiler of which the power can vary from 0 to 3 kW. The flow rate of superheated vapor generated by the evaporator is adjusted by another by-pass valve at the outlet of evaporator. The vapor passes through the adiabatic section to come out in a saturated/superheated condition. It is then condensed in the test section to a saturated condition. Transparent tubes are connected to both ends of the test section to visually inspect the vapor conditions. The outlet condensate flows through the sub-cooling section to reach a subcooled condition and comes into the volumetric cylinder to read the volumetric flow rate. Finally, it is collected to the liquid receiver.

The cooling water loop designed for condensing the vapor contains a water thermostat bath with a pump and the adjustable temperature from 40 to 100°C. A by-pass valve is also provided to adjust the flow rate. Varying the temperature and flow rate of cooling water, we can expect different vapor quality at the outlet of test section for a fixed inlet vapor Reynolds number. The flow rate of cooling water is measured by weighing the cooling water collected in a certain time.

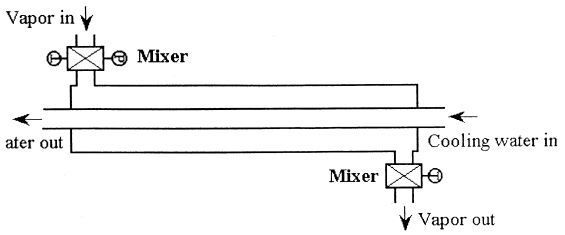

Fig. 3. Details of test section.

The test section is really a tube-in-tube condenser with counterflow arrangement, which is 300 mm in length. The outer tube of the condenser is 11.97 mm i.d. and is covered by a layer of insulation outside. The inlet vapor through a mixer, flows into the annulus and is condensed along the outside surface of the inner tube, while the cooling water flows into the test tube in the opposite direction, as shown in Fig. 3. Two types of annulus are selected as test section with the same outer tube but different inner tube of 2.97 mm o.d. and 5.98 mm o.d., signed by Type A and Type B, respectively.

At the both ends of the total test section, the temperatures of vapor/condensate were measured. The inlet and outlet temperatures of cooling water of the condenser and the condensate temperature in volumetric cylinder were also measured. All the temperatures were measured by the 0.1 mm T-type copper–constantan thermocouples calibrated with an accuracy of 0.1°C. The pressures were measured by pressure gauge with an accuracy of ±0.25%. The weighing accuracy of cooling water is 0.5 g, while the accuracy of volumetric cylinder is 0.1 ml.

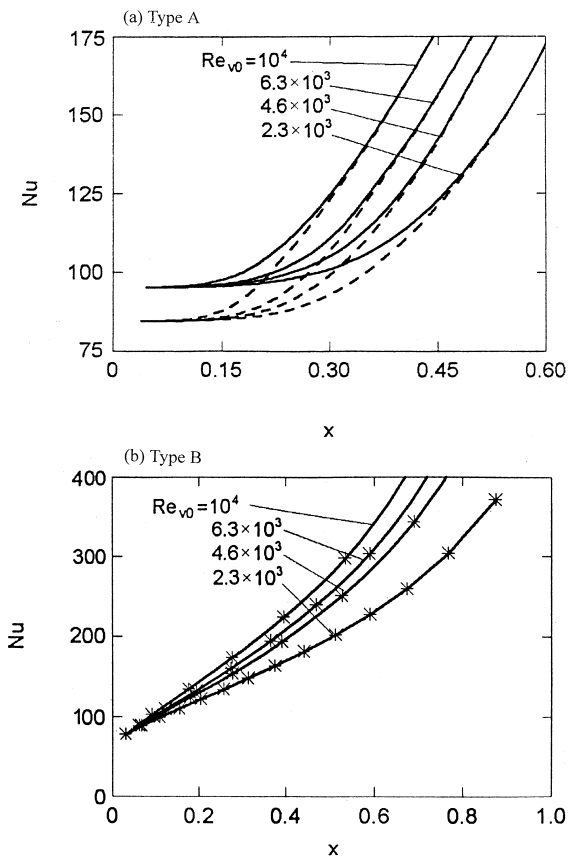

Fig. 4. Plot of predicted Nu vs vapor quality, x.

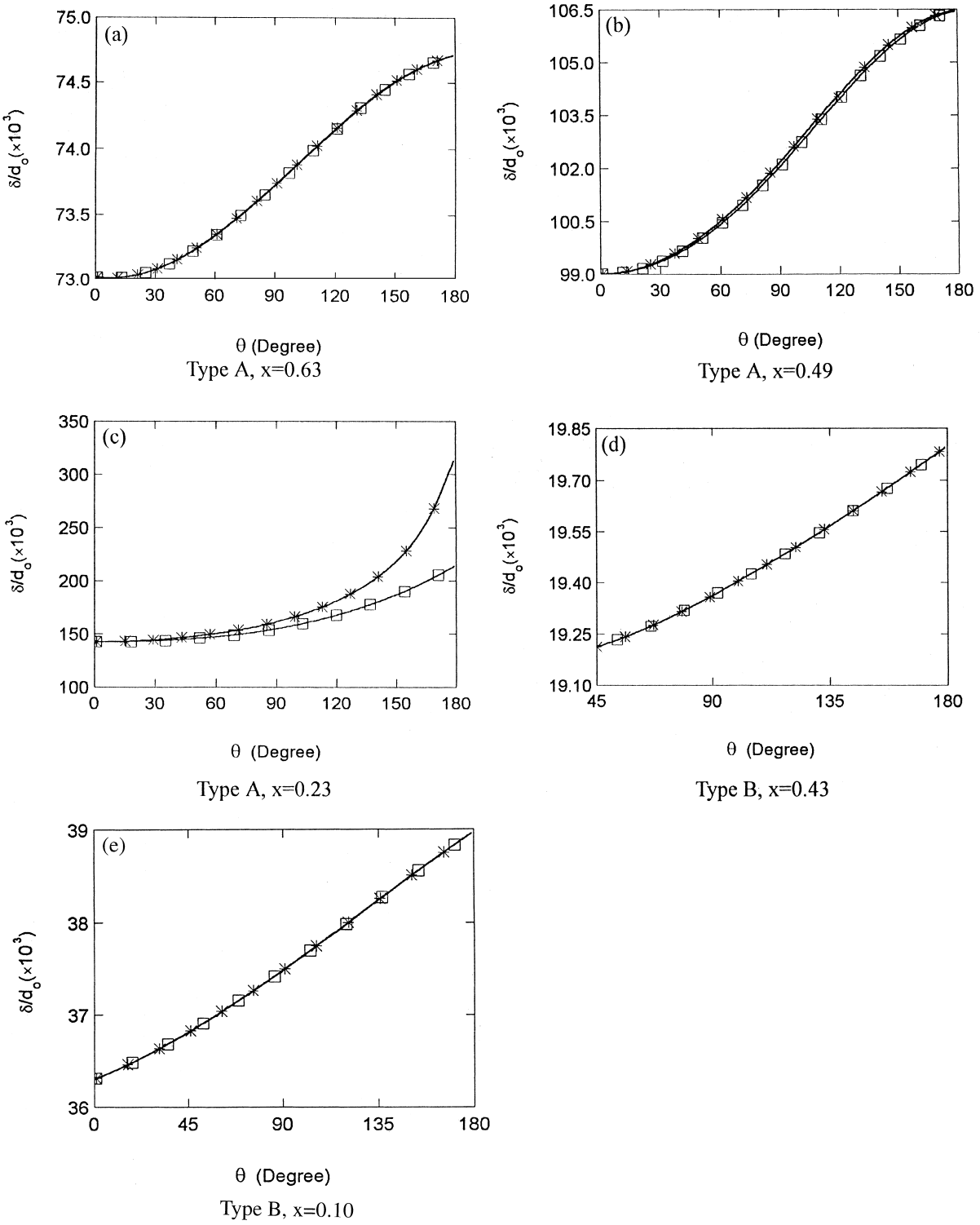

Fig. 5. Variation of condensate film thickness along circumference of inner tube, $Re_{v0} = 6.3 \times 10^3$.

Taking the arithmetic mean of inlet and outlet cooling water temperatures as its average value, $\bar{t}_{cool}$, and the arithmetic mean of vapor temperature at both ends of test section as vapor temperature, t_s, we can obtain the average condensation heat transfer coefficient $\bar{\alpha}_{exp}$ for the test section as

$$\frac{1}{\bar{\alpha}_{exp}} = \frac{t_s - \bar{t}_{cool}}{q} = \frac{d_o}{2\lambda_w} \ln\frac{d_o}{d_i} - \frac{d_o}{d_i}\frac{1}{\alpha_{cool}} \tag{25}$$

where α_{cool} is the convective heat transfer coefficient of cooling water in inner tube, calculated by Dittus–Boelter correlation. The average Nusselt number can be thereby acquired by

$$\overline{Nu}_{exp} = \bar{\alpha}_{exp}\, d_o/\lambda_l. \tag{26}$$

Before the tests started, the outer wall of the test tube was treated with mechanical polishing and the inner wall of the tube was washed by acetone repeatedly to avoid organic and dirt contamination. At most test conditions, the error of heat balance between sensible heat of cooling water and latent heat of condensate is less than 5%. For the uncertainty analysis, the basic methodology of Kline and McClintock [14] was adopted. From the analysis, the estimated average uncertainty in the measurement of the present experiments for Nu was $\pm 25\%$.

4. Results and discussions

For carrying out a concrete analysis, we considered the case of flow condensation of steam with inlet vapor Reynolds numbers, Re_{v0}, from 2300 to 10^4. The analytical predicting results are illustrated in Figs. 4 and 5.

The Nusselt number, Nu, for flow condensation heat transfer through annulus of both Type A and Type B with different inlet Reynolds numbers, are plotted as function of vapor quality, x, in Fig. 4. The results with neglecting the effect of surface tension on vapor–liquid interface are given simultaneously for comparison. According to Eq. (7), the effect of surface tension is mainly embodied by the additional capillary pressure drop due to the film thickness varied along circumference of tube. The degree of this effect is determined by the condensate film curvature and variation of film thickness. For annulus of Type A, in which vapor is condensed on a small-diameter tube, the condensate film curvature become obvious as compared with the tube diameter, especially in lower vapor quality zone, $x \leq 0.45$. Also for small-diameter tube, the bending of condensate film makes more liquid drained by gravity along periphery, which leads to the film accumulating, and hence, the variation of film thickness is enhanced too. Therefore, an obvious deviation exists for neglecting surface tension shown in Fig. 4(a). However, for annulus of Type B with larger outside diameter of inner tube, the variation of condensate film curvature does not actually influence the condensation process yet, so neglecting the capillary pressure drop due to surface tension almost has no effect on Nu.

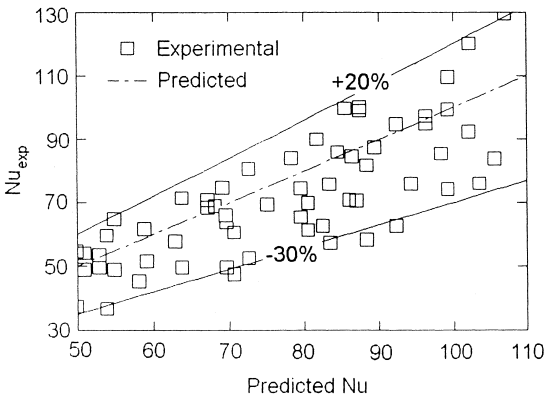

Fig. 6. Comparison of predicted value with experimental data.

As the effect of shear stress on phase-change interface enhances with increasing Re_{v0}, more important role of shear stress would be expected for thinning the condensate film thickness, and hence, Nu will increase. However, the film thickness increases rapidly with decreasing x due to condensate accumulation. This may lead to the case shown in Fig. 5(c), where the thermal resistance comes dominantly from the condensate film layer, and so, there will be little influence on Nu for different Re_{v0}.

It is well known that, both the shear stress and the surface tension on vapor–liquid interface can promote the condensate distributing more uniformly along tube circumference. Therefore, for flow condensation of vapor in horizontal annulus, the increasing shear stress on vapor–liquid interface will improve accordingly the condensate film thickness distribution more even along the inner tube periphery. This can be illustrated, at different vapor quality, x, for Type B compared with that for Type A, as shown in Fig. 5. For annulus of Type A with small-diameter of inner tube, the shear stress decreases with decreased quality, thereby, the surface tension will take more obvious effect in distributing the film thickness uniformly at low quality zone.

Fig. 6 shows the comparison of the predicted average Nu number from analytical model with the experimental results. It indicates that most of the experimental values are within a range of -30% to $+20\%$ of the predicted values. As the estimated uncertainty of the present experimental measurement of Nu_{exp} is about $\pm 25\%$, the deviation of predicted and

experimental results may indicate a little over-prediction of the analytical model.

5. Conclusions

An analytical model, taking into account the effect of surface tension on the nature of flow condensation on the outside surface of a small/mini diameter tube is proposed.

For traditional industrial tube of which the diameter is larger than about 6 mm, the surface tension has actually negligible effect on Nusselt number for flow condensation and distribution of condensate film along the tube surface. However, for small/mini tube of outside diameter less than 3 mm, the effect of surface tension could not be neglected, especially in low vapor quality zone.

In horizontal annulus, both the shear stress and surface tension influence the flow condensation by means of distributing condensate film uniformly along tube circumference. Comparison with the experimental data verifies the proposed analytical model to some extent.

Acknowledgements

The financial support for this research from the National Natural Science Foundation of China (Grant No. 59995550-3) is greatly acknowledged.

References

[1] W. Nusselt, Die Oberflächenkondensation des Wasserdampfes, Ver Deut. Ing. 60 (1916) 541–546.
[2] J.W. Rose, Effect of pressure gradient in force convection film condensation on a horizontal tube, Int. J. Heat Mass Transfer 27 (1984) 39–47.
[3] K. Suzuki, Y. Hagiwara, H. Izumi, A numerical study of forced-convective filmwise condensation in a vertical tube, JSME Int. J., Ser. II 33 (1990) 134–140.
[4] W.M. Rohsenow, J.H. Weber, A.T. Ling, Effect of vapor velocity on laminer and turbulent-film condensation, Trans. ASME 78 (1956) 1637–1643.
[5] W.M. Rohsenow, Film condensation, Applied Mechanics Reviews 23 (1970) 487–496.
[6] S. Hirasawa, K. Hijikata, Y. Mori, W. Nakayama, Effect of surface tension on condensate motion in laminer film condensation (study of liquid film in a small trough), Int. J. Heat Mass Transfer 23 (1980) 413–418.
[7] M. Yanadori, K. Hijikata, Y. Mori, M. Uchida, Fundamental study of laminar film condensation heat transfer in a downward horizontal surface, Int. J. Heat Mass Transfer 28 (1985) 1937–1944.
[8] S.B. Memory, V.H. Adams, P.J. Marto, Free and force convection laminar film condensation on horizontal elliptical tubes, Int. J. Heat Mass Transfer 40 (1997) 3395–3406.
[9] R. Krupiczka, Effect of surface tension on laminar film condensation on a horizontal cylinder, Chem. Eng. Process. 19 (1985) 199–203.
[10] V.M. Buznik, V.A. Aleksandrov, G.A. Smirnov, The effect of surface-tension forces on the heat-transfer coefficient in the condensation of vapors on inclined tubes, Int. Chem. Eng. 9 (1969) 216–219.
[11] A.M. Jacobi, V.W. Goldschmidt, The effect of surface tension variation on filmwise condensation and heat transfer on a cylinder in cross flow, Int. J. Heat Mass Trans. 32 (1989) 1483–1490.
[12] W.H. Henstock, T.J. Hodgson, The interfacial drag and height of the wall layer in annular flows, AIChE J. 22 (1976) 990–1000.
[13] A. Faghri, L.C. Chow, Annular condensation heat transfer in a micro-gravity environment, Int. Comm. Heat Mass Trans. 18 (1991) 715–792.
[14] S.J. Kline, F.A. McClintock, Describing uncertainties in single-sample experiments, Mech. Engng 75 (1953) 3–12.